

Out of Equilibrium Non-perturbative Quantum Field Dynamics in Homogeneous External Fields

F. J. Cao, H. J. de Vega

LPTHE, Université Pierre et Marie Curie (Paris VI) et
Denis Diderot (Paris VII), Tour 16, 1er. étage, 4, Place Jussieu,
75252 Paris, Cedex 05, France

October 27, 2018

Abstract

The quantum dynamics of the symmetry broken $\lambda(\vec{\Phi}^2)^2$ scalar field theory in the presence of an homogeneous external field is investigated in the large N limit. We choose as initial state the ground state for a constant external field $\vec{\mathcal{J}}$. The sign of the external field is suddenly flipped from $\vec{\mathcal{J}}$ to $-\vec{\mathcal{J}}$ at a given time and the subsequent quantum dynamics calculated. Spinodal instabilities and parametric resonances produce large quantum fluctuations in the field components transverse to the external field. This allows the order parameter to turn around the maximum of the potential for intermediate times. Subsequently, the order parameter starts to oscillate near the global minimum for external field $-\vec{\mathcal{J}}$, entering a novel quasi-periodic regime.

PACS: 11.10.-z, 11.15.Pg, 11.30.Qc

Contents

1	Introduction	2
2	Classical field dynamics	3
2.1	Classical evolution equation and initial conditions	3
2.2	The classical dynamics	6

3	Quantum field dynamics	7
3.1	Quantum equations of motion and initial conditions	7
3.2	Early time quantum evolution	9
3.2.1	$j > j_c$	10
3.2.2	$j < j_c$	10
3.3	Intermediate time quantum evolution	11
3.4	Constraints on the trajectory due to the conservation of the energy	14
4	Comments and Conclusions	15
5	Acknowledgements	16
6	Appendix	16
6.1	Appendix A: Spinodal instability	16
6.2	Appendix B: Ground state results	18

1 Introduction

The understanding of the physics at large energy density situations is fundamental to achieve a proper picture both for ultrarelativistic heavy ion collisions [1] and for the early universe [2, 3, 4]. These physical phenomena cannot be treated with the usual quantum field perturbation methods and call for self-consistent nonperturbative methods as the large N approach and Hartree approximations [2, 3, 4, 5, 7, 8].

Here, we study effects of external fields in non-perturbative quantum field dynamics using the large N limit method.

The effective potential of the $O(N)$ $\lambda \Phi^4$ theory with broken symmetry has two degenerate minima for zero external field. In the presence of a small uniform external field $\vec{\mathcal{J}}$ the potential becomes tilted and the degeneracy between the minima lifted. The absolute minimum becomes the vacuum while the other local minimum becomes a metastable vacuum. See Fig. 1.

We take as initial state the ground state. That is, the field expectation value is initially at the absolute minimum and the field modes are in the vacuum. Then, at a given time we change the sign of the external field: $\vec{\mathcal{J}} \rightarrow -\vec{\mathcal{J}}$. Flipping the sign of the external field exchanges the local minima. That is, the absolute minimum becomes the false vacuum and viceversa. As a consequence, the system is now near the false vacuum. Spinodal resonances develop and the fluctuations transverse to the direction of $\vec{\mathcal{J}}$ grow exponentially till they are shut-off by the non-linear back-reaction. The expectation value of the field tends to reach the absolute minimum which is on the other side of a potential barrier for values $|\vec{\mathcal{J}}|$ smaller than $\frac{2}{\sqrt{27}} (|m|^3 \sqrt{\frac{2}{\lambda}})$. See Fig. 1.

There are two regimes for the dynamics separated by a critical value of the external field $J_c = \sqrt{2 \frac{(13^2+15\sqrt{5})}{19^3}} (|m|^3 \sqrt{\frac{2}{\lambda}})$:

For $|\vec{\mathcal{J}}| > J_c$ the system quickly reaches a quasiperiodic regime where the field expectation value oscillates near the true quantum vacuum. See Figs. 2, 3, 4 and 5.

For $|\vec{\mathcal{J}}| < J_c$ the field cannot reach the absolute minimum moving in the longitudinal direction except by tunnel effect which is suppressed in the large N limit. Instead, the field turns around the potential maximum developing large transverse quantum fluctuations $\mathcal{O}(m^2/\lambda)$. It takes a time $t_s \sim \frac{1}{\sqrt{J}m} \log \frac{1}{\lambda}$ (spinodal time) for the quantum fluctuations to become of the order $\mathcal{O}(m^2/\lambda)$. By this time the field expectation value makes a spectacular jump and starts to oscillate near the true vacuum. See Figs. 6, 7 and 8.

For later times the evolution in both cases becomes quasiperiodic showing a clear separation between fast and slow variables. The fast time dependence of the field expectation value is explicitly found in terms of elliptic Jacobi functions. Comparison with the full numerical solution shows that their parameters exhibit slow time dependence. The smaller is $|\vec{\mathcal{J}}|$ the slower are the slow variables. We also see that the mass squared is of order $|\vec{\mathcal{J}}|$. For $|\vec{\mathcal{J}}| = 0$ we recover the known zero external field results [5, 7].

We consider small values of the coupling constant $\lambda \ll 1$ in order to separate the different time scales of the evolution.

2 Classical field dynamics

We will first propose and solve the problem in classical field theory, in order to present results that will be used later for comparison. We consider the classical $O(N)$ -invariant scalar field model with quartic self-interaction [8] in the presence of an homogeneous external field $\vec{\mathcal{J}}$. We study in this model the evolution of the ground state after the change $\vec{\mathcal{J}} \rightarrow -\vec{\mathcal{J}}$ in the external field.

2.1 Classical evolution equation and initial conditions

The action and Lagrangian density are given by,

$$\begin{aligned} S &= \int d^4x \mathcal{L} , \\ \mathcal{L} &= \frac{1}{2} [\partial_\mu \vec{\Phi}(x)]^2 - \frac{1}{2} m^2 \vec{\Phi}^2 - \frac{\lambda}{8N} (\vec{\Phi}^2)^2 + \vec{\mathcal{J}} \cdot \vec{\Phi} . \end{aligned} \quad (1)$$

We restrict ourselves to a translationally invariant situation. In this case the field $\vec{\Phi}$ and the external field $\vec{\mathcal{J}}$ are independent of the spatial coordinates \vec{x} and only depend on time. The evolution equation is then

$$\ddot{\vec{\Phi}}(t) + \left(m^2 + \frac{\lambda}{2N} \vec{\Phi}^2(t) \right) \vec{\Phi}(t) = \vec{\mathcal{J}}(t) \quad (2)$$

and the classical potential

$$V(\vec{\Phi}) = \frac{1}{2} m^2 \vec{\Phi}^2 + \frac{\lambda}{8N} (\vec{\Phi}^2)^2 - \vec{\mathcal{J}} \cdot \vec{\Phi} . \quad (3)$$

We consider the broken symmetry case ($m^2 < 0$).

Choosing the first axis of the internal space in the direction of the external field $\vec{\mathcal{J}}$, their components are $\vec{\mathcal{J}} = (\sqrt{N}J, 0, \dots, 0)$. Consequently, the $\vec{\Phi}$ field can be expressed as $\vec{\Phi} = (\sqrt{N}\phi, \vec{\phi}_\pi)$.

Thus, the potential becomes:

$$\begin{aligned} V(\vec{\Phi}) &= N V_J(\phi) + V_\pi(\vec{\phi}_\pi) \\ V_J(\phi) &= \frac{1}{2} m^2 \phi^2 + \frac{\lambda}{8} \phi^4 - J \phi \\ V_\pi(\phi, \vec{\phi}_\pi) &= \frac{1}{2} m^2 \vec{\phi}_\pi^2 + \frac{\lambda}{8N} \left[2 \phi^2 \vec{\phi}_\pi^2 + \left(\vec{\phi}_\pi^2 \right)^2 \right] . \end{aligned} \quad (4)$$

We choose the *ground state as initial state*, therefore it has the form (this can be shown from the previous expressions)

$$\begin{aligned} \phi(t_i) &= \phi_0 \quad ; \quad \dot{\phi}(t_i) = 0 \\ \vec{\phi}_\pi(t_i) &= 0 \quad ; \quad \dot{\vec{\phi}}_\pi(t_i) = 0 \end{aligned} \quad (5)$$

where ϕ_0 is the global minimum of $V_J(\phi)$.

The evolution equations for $\vec{\phi}_\pi$ are

$$\ddot{\vec{\phi}}_\pi(t) + \left[m^2 + \frac{\lambda}{2N} \left(\phi^2(t) + \vec{\phi}_\pi^2(t) \right) \right] \vec{\phi}_\pi(t) = 0 , \quad (6)$$

and with the previous initial conditions, *independently* of the value of J , the solution is simply

$$\vec{\phi}_\pi(t) = 0 . \quad (7)$$

Therefore, the *classical* problem reduces to the following *one component* field problem. The evolution equation for ϕ reduces to

$$\ddot{\phi}(t) + \left[m^2 + \frac{\lambda}{2} \phi^2(t) \right] \phi(t) = +J \quad \text{for } t < 0 . \quad (8)$$

As it is obvious, the ground state ϕ_0 is a constant solution of this equation. We see from Eq. (4) that ϕ_0 , the global minimum of $V_J(\phi)$ fulfills Eq. (8).

We introduce the dimensionless variables

$$\tau \equiv |m| t \quad ; \quad \eta \equiv \sqrt{\frac{\lambda}{2|m|}} \phi \quad , \quad j \equiv \sqrt{\frac{\lambda}{2|m|^3}} J \quad , \quad V_{\tau \leq 0} \equiv \frac{\lambda}{2m^4} V_J \quad , \quad \vec{j} \equiv \sqrt{\frac{\lambda}{2N|m|^3}} \vec{\mathcal{J}} . \quad (9)$$

Therefore,

$$V_{\tau \leq 0}(\eta) = -\frac{1}{2}\eta^2 + \frac{1}{4}\eta^4 - j\eta,$$

since we choose $m^2 < 0$.

Thus, the classical vacua are the solutions of the cubic equation $V'_{\tau \leq 0}(\eta) = 0$,

$$\eta^3 - \eta - j = 0 \quad (10)$$

For small external fields $j < \frac{2}{\sqrt{27}} = 0.3849002 \dots$ Eq. (10) has three real roots. The ground state (the global minimum) of the potential $V_{\tau \leq 0}$ is at

$$\eta = \eta_0 \equiv \frac{2}{\sqrt{3}} \cos \left[\frac{1}{3} \arccos \left(\frac{\sqrt{27}j}{2} \right) \right] = 1 + \frac{1}{2}j - \frac{3}{8}j^2 + \frac{1}{2}j^3 - \frac{105}{128}j^4 + O(j^5), \quad (11)$$

there is a local minimum (false vacuum) at

$$\eta_{fv} \equiv \frac{2}{\sqrt{3}} \cos \left[\frac{1}{3} \arccos \left(\frac{\sqrt{27}j}{2} \right) + \frac{2\pi}{3} \right] = -1 + \frac{1}{2}j + \frac{3}{8}j^2 + \frac{1}{2}j^3 + \frac{105}{128}j^4 + O(j^5),$$

and a local maximum at

$$\eta_M \equiv \frac{2}{\sqrt{3}} \cos \left[\frac{1}{3} \arccos \left(\frac{\sqrt{27}j}{2} \right) + \frac{4\pi}{3} \right] = -j - j^3 + O(j^5) \quad (12)$$

For larger external fields $j > \frac{2}{\sqrt{27}}$ there is only one real minimum, (the absolute minimum) at

$$\begin{aligned} \eta = \eta_0 &\equiv \left(\frac{j}{2} \right)^{1/3} \left[\left(1 + \sqrt{1 - \frac{4}{27j^2}} \right)^{1/3} + \left(1 - \sqrt{1 - \frac{4}{27j^2}} \right)^{1/3} \right] \\ &= j^{1/3} + \frac{1}{3j^{1/3}} - \frac{1}{81j^{5/3}} + O(j^{-7/3}). \end{aligned}$$

We shall concentrate in the more interesting case $j < \frac{2}{\sqrt{27}}$.

The field stays in the ground state η_0 with $j > 0$ from the (negative) initial time τ_i till $\tau = 0$. At $\tau = 0$ we suddenly flip the sign of the external field j .

That is, the time dependence of the external field is

$$\vec{j} = \begin{cases} (j, 0, \dots, 0) & \text{for } \tau \leq 0 \\ (-j, 0, \dots, 0) & \text{for } \tau > 0 \end{cases} \quad (13)$$

This change of sign of j introduces some amount of energy in the system.

As previously stated this problem reduces to a one component field problem. Therefore, the potential is given in dimensionless variables by (see Fig. 2, 6)

$$V(\eta) = \begin{cases} V_{\tau \leq 0}(\eta) &\equiv -\frac{1}{2}\eta^2 + \frac{1}{4}\eta^4 - j\eta & \text{for } \tau \leq 0 \\ V_{\tau > 0}(\eta) &\equiv -\frac{1}{2}\eta^2 + \frac{1}{4}\eta^4 + j\eta & \text{for } \tau > 0 \end{cases} \quad (14)$$

The equation of motion for $\tau > 0$ is

$$\ddot{\eta} + (-1 + \eta^2) \eta = -j, \quad (15)$$

where $-1 + \eta^2$ plays the role of an effective mass. The initial state at $\tau = 0$ is the ground state for $\tau \leq 0$, and it has the form

$$\eta(0) = \eta_0 \quad ; \quad \dot{\eta}(0) = 0. \quad (16)$$

2.2 The classical dynamics

We have shown above that the initial state (the ground state for an external field j) is a stationary state of the evolution equations for $\tau \leq 0$. The change $j \rightarrow -j$ at $\tau = 0$ breaks this stationarity and the system now finds itself near a metastable state (see Fig. 2, 6). We consider $j < \frac{2}{\sqrt{27}}$ when there is a potential barrier (see Fig. 1). This change in the sign of the external field j , increases the energy density of the system by an amount $V_{\tau>0}(\eta_0) - V_{\tau\leq 0}(\eta_0) = 2j\eta_0$. However, even if the field is near the metastable minimum, it could have now enough energy to jump above the barrier and reach the global minimum of the potential. As the height of the barrier is $V_{\tau>0}(\eta_{M'})$ the condition to jump above the barrier is

$$V_{\tau>0}(\eta_0) > V_{\tau>0}(\eta_{M'}), \quad (17)$$

where $\eta_{M'}$ is the local maximum of the potential $V_{\tau>0}(\eta)$.

Solving this equation one obtains that the field jumps above the barrier provided $|j| > j_c$ with

$$j_c = \sqrt{2 \frac{(13^2 + 15\sqrt{5})}{19^3}} = 0.243019 \dots \quad (18)$$

[Notice that $j_c < \frac{2}{\sqrt{27}}$ and therefore there is indeed a barrier for these values $j \leq j_c$.]

This critical value j_c of the external field separates the dynamics in two regimes

- $|j| > j_c$. The field jumps above the barrier and reaches the region of the global minimum. After this the field continues to jump above the barrier back and forth with periodic oscillations. See Fig. 2 and dashed line in Fig. 3.
- $|j| < j_c$. The system does *not* jump above the barrier, and oscillates periodically between the turning points of the motion η_0 and η_t around the metastable minimum. η_0 is given by Eq. (11) and η_t is the solution of the equation

$$V_{\tau>0}(\eta_t) = V_{\tau>0}(\eta_0)$$

we find,

$$\eta_t = 1 - \frac{3}{2}j - \frac{11}{8}j^2 - \frac{7}{2}j^3 - \frac{1049}{128}j^4 + O(j^5) \quad (19)$$

Since both η_t and η_0 are positive, η is always positive. See Fig. 6 and dashed line in Fig. 7.

3 Quantum field dynamics

In this section we derive the quantum equation of motion and compute the quantum field dynamics using the large N limit. As in the previous section, we consider the $O(N)$ -invariant scalar field model with quartic self-interaction [8] in the presence of an homogeneous external field $\vec{\mathcal{J}}$. We study in this model the evolution of the ground state after the change $\vec{\mathcal{J}} \rightarrow -\vec{\mathcal{J}}$ in the external field.

3.1 Quantum equations of motion and initial conditions

The action and Lagrangian density are,

$$\begin{aligned} S &= \int d^4x \mathcal{L} , \\ \mathcal{L} &= \frac{1}{2} [\partial_\mu \vec{\Phi}(x)]^2 - \frac{1}{2} m^2 \vec{\Phi}^2 - \frac{\lambda}{8N} (\vec{\Phi}^2)^2 + \vec{\mathcal{J}} \cdot \vec{\Phi} \end{aligned} \quad (20)$$

where $\vec{\Phi}$ is now a quantum operator.

We restrict ourselves to a translationally invariant situation. In this case the order parameter $\langle \vec{\Phi}(\vec{x}, t) \rangle$ and the external field $\vec{\mathcal{J}}(\vec{x}, t)$ are independent of the spatial coordinates \vec{x} and only depend on time. Moreover, we choose the direction of $\vec{\mathcal{J}}(t)$ independent of time. Then, we can choose this direction as the first axis in the N -dimensional internal space.

$$\vec{\mathcal{J}} = \begin{cases} (J, 0, \dots, 0) & \text{for } t \leq 0 \\ (-J, 0, \dots, 0) & \text{for } t > 0 \end{cases} . \quad (21)$$

The field expectation value in the problem we are studying is parallel to the external field:

$$\vec{\Phi}(x) = (\sigma(x), \vec{\pi}(x)) = (\sqrt{N}\phi(t) + \chi(x), \vec{\pi}(x)) \quad (22)$$

with $\phi(t) = \langle \sigma(x) \rangle$; thus, $\langle \chi(x) \rangle = 0$. While in the $N - 1$ directions transversal to the expectation value we have $\langle \vec{\pi}(\vec{x}, t) \rangle = 0$.

The derivation of the equations of motion in the large N limit in this case, is analogous to the case without external field, that has been explained in detail in [8]. Thus, we will only present here the main concepts and equations.

We have one direction parallel to the expectation value, and $N - 1$ transversal directions. The transverse fluctuations dominate in the large N limit while the longitudinal fluctuations only contribute to the $1/N$ corrections to the equations of motion.

The evolution equation for the expectation value is for $t > 0$

$$\ddot{\phi}(t) + \left\{ m^2 + \frac{\lambda}{2} \left[\phi^2(t) + \frac{\langle \vec{\pi}^2(x) \rangle}{N} \right] \right\} \phi(t) = -J \quad (23)$$

where the dot denotes the time derivative. We see in the previous equation that

$$\mathcal{M}_d^2(t) \equiv m^2 + \frac{\lambda}{2} \left[\phi^2(t) + \frac{\langle \vec{\pi}^2(x) \rangle}{N} \right]$$

plays the role of an effective mass. The last term in $\mathcal{M}_d^2(t)$ has a quantum origin and it is absent in the classical effective mass. It can be interpreted as an in-medium effect due to the presence of $\vec{\pi}$ particles.

In the Heisenberg picture we can write

$$\vec{\pi}(\vec{x}, t) = \int \frac{d^3\vec{k}}{\sqrt{2}(2\pi)^3} \left[\vec{a}_k \varphi_k(t) e^{i\vec{k}\cdot\vec{x}} + \vec{a}_k^\dagger \varphi_k^*(t) e^{-i\vec{k}\cdot\vec{x}} \right] \quad (24)$$

where \vec{a}_k , \vec{a}_k^\dagger are the time independent annihilation and creation operators with the usual canonical commutation relations. Thus, the $\varphi_k(t)$ are the mode functions of the field and we can express $\langle \vec{\pi}^2(x) \rangle$ as

$$\begin{aligned} \frac{\langle \vec{\pi}^2(x) \rangle}{N} &= \frac{1}{2} \int \frac{d^3k}{(2\pi)^3} \left[|\varphi_k(t)|^2 - \mathcal{S}_d \right] . \\ \mathcal{S}_d &= \frac{1}{k} - \frac{\theta(k - \kappa)}{2k^3} \mathcal{M}_d^2(t) \end{aligned} \quad (25)$$

where κ is an arbitrary renormalization scale, and we will choose $\kappa = |m_R|$ for simplicity. (For details on the renormalization procedure, that leads to the subtraction \mathcal{S}_d see Ref. [5].)

In the previous expressions we have written k , instead of \vec{k} , since we choose spherically symmetric initial conditions.

The mode functions have the following evolution equations

$$\ddot{\varphi}_k(t) + \omega_k^2(t) \varphi_k(t) = 0 \quad , \quad \omega_k^2(t) \equiv k^2 + \mathcal{M}_d^2(t) . \quad (26)$$

We consider values of the field $|J| < \frac{2}{\sqrt{27}} (|m|^3 \sqrt{\frac{2}{\lambda}})$ where the potential V_J has two local minima. As initial state we take the ground state for $t \leq 0$

$$\begin{aligned} \phi(0) &= \phi_0 \quad ; \quad \dot{\phi}(0) = 0 \\ \varphi_k(0) &= \frac{1}{\sqrt{\omega_k(0)}} \quad ; \quad \dot{\varphi}_k(0) = -i \sqrt{\omega_k(0)} . \end{aligned} \quad (27)$$

where ϕ_0 is the global minimum of $V_J(\phi)$ [defined in Eqs. (9) and (11)] and $\omega_k(0) = \sqrt{k^2 + m^2 + (\lambda/2)\phi_0^2}$ (the square root is real for all k , because $m^2 + (\lambda/2)\phi_0^2 > 0$). These initial conditions correspond to the quantum vacuum (no excitations).

It is convenient to introduce the following dimensionless quantities [in addition to those in Eq. (9)],

$$\begin{aligned} q &\equiv \frac{k}{|m|} \quad ; \quad g \equiv \frac{\lambda}{8\pi^2} \quad ; \quad \mathcal{M} \equiv \frac{\mathcal{M}_d}{|m|} \quad ; \\ \varphi_q(\tau) &\equiv \sqrt{|m|} \varphi_k(t) \quad ; \quad g\Sigma(\tau) \equiv \frac{\lambda}{2|m|^2} \langle \pi^2(t) \rangle \quad ; \end{aligned} \quad (28)$$

where m and λ stand for the renormalized mass of the inflaton and the renormalized self-coupling, respectively [2, 3].

The quantum evolution equation in dimensionless variables are then for $\tau > 0$,

$$\ddot{\eta}(\tau) + \mathcal{M}^2(\tau) \eta(\tau) = -j \quad ; \quad \ddot{\varphi}_q(\tau) + \omega_q^2(\tau) \varphi_q(\tau) = 0 \quad (29)$$

with

$$\begin{aligned} \mathcal{M}^2(\tau) &= -1 + \eta^2(\tau) + g\Sigma(\tau) \quad ; \quad \omega_q^2 = q^2 + \mathcal{M}^2(\tau) \\ g\Sigma(\tau) &= g \int q^2 dq \left[|\varphi_q(\tau)|^2 - \mathcal{S}(\tau) \right] \quad ; \quad \mathcal{S}(\tau) = \frac{1}{q} - \frac{\theta(q-1)}{2q^3} \frac{\mathcal{M}_d^2(\tau)}{|m|^2}. \end{aligned} \quad (30)$$

And the initial conditions are

$$\begin{aligned} \eta(0) &= \eta_0 \quad ; \quad \dot{\eta}(0) = 0 \\ \varphi_q(0) &= \frac{1}{\sqrt{\omega_q(0)}} \quad ; \quad \dot{\varphi}_q(0) = -i \sqrt{\omega_q(0)}. \end{aligned} \quad (31)$$

where η_0 is given by Eq. (11); and $\omega_q(0) = \sqrt{q^2 - 1 + \eta_0^2}$ because the initial conditions imply $g\Sigma(0) = O(g) \ll 1$. (ω_q is real for all q , because $\eta_0^2 > 1$).

It is important to note that the quantum effective mass equals the classical effective mass plus an additional quantum term, $g\Sigma(\tau)$. This term comes from the in-medium effects due to the presence of $\vec{\pi}$ particles.

In this section we have exposed the quantum equations of motion and the initial conditions using the Heisenberg picture. The equations shown for the large N limit are the same as those obtained in the Schrödinger picture with a gaussian *ansatz* for the wave functional (as it has been shown in Refs. [5, 9])

$$\Psi[\vec{\pi}; \tau] = \mathcal{N}_\Psi \prod_{\vec{q}} e^{-\frac{A_{\vec{q}}(\tau)}{2} \vec{\pi}_{\vec{q}} \cdot \vec{\pi}_{-\vec{q}}} \quad (32)$$

where \mathcal{N}_Ψ is the normalization factor. The relation between the two pictures is made explicit by using the relation $A_q = -i \dot{\varphi}_q^* / \varphi_q^*$.

$g\Sigma(\tau)$ gives us the spreading of this wave functional, as we see from Eq. (28) (the expectation values are independent of the picture).

3.2 Early time quantum evolution

At early times, $g\Sigma(\tau)$ is negligible in the η evolution equation because $g\Sigma(0) = O(g) \ll 1$. Thus, for early times the quantum dynamics of the expectation value $\eta(\tau)$ is the same as the dynamics of the classical field presented in section 2. This has been explicitly verified from the numerical solution of the full quantum equations (29)–(31). As in the classical case, we can distinguish two dynamical regimes depending on the value of j compared with j_c .

Later on, this picture is modified due to the effects of the spinodal instabilities and parametric resonances. They make the quantum modes to grow, and therefore so does $g\Sigma(\tau)$. Parametric resonances arrive because $\mathcal{M}^2(\tau)$ oscillates in time. In addition, the modes grow exponentially (spinodal instabilities) in the time intervals where $\mathcal{M}^2(\tau) < 0$.

These effects have a quantum nature, and they change the dynamics of the expectation value $\eta(\tau)$, due to its coupling with the quantum modes through $g\Sigma(\tau)$. $g\Sigma(\tau)$ gives the spreading of the field wave functional in the transverse directions as shown by Eq. (28) (recall that the transverse fields have zero expectation value).

We comment below on the effects of this phenomena in the dynamics.

3.2.1 $j > j_c$

For early times the dynamics of the field expectation value is the same as in the classical case. Thus, the system in this case has enough energy to jump above the barrier and reach the region of the global minimum of the potential (see Fig. 2). The system continues to jump above the barrier back and forth until the effects of the quanta created through spinodal instability and parametric resonance become important, i.e., $g\Sigma(\tau) \sim 1$ (see Figs. 3–5).

The system is spinodally unstable when $\mathcal{M}^2(\tau) < 0$, i.e., for $\eta^2(\tau) + g\Sigma(\tau) < 1$, that for early times ($g\Sigma \simeq 0$) reduces to $|\eta(\tau)| < 1$. It also has parametric resonances due to the oscillations of $\mathcal{M}^2(\tau)$. Both mechanisms lead to an abundant creation of quanta transferring energy from the η degree of freedom to the quantum fluctuations $\varphi_k(\tau)$. Therefore, $g\Sigma(\tau)$ increases while the amplitude of the oscillations of $\eta(\tau)$ decreases. See Figs. 3 and 4.

3.2.2 $j < j_c$

The early dynamics is the same as in the classical treatment. For $j < j_c$ the system does not have enough energy to jump above the barrier and reach the global minimum, and it oscillates around the metastable minimum (false vacuum). (See Fig. 6).

The field could go classically to the global minimum region moving in the transverse directions. But this possibility is excluded due to the initial conditions Eq. (5): the transverse field components and its derivatives are zero and they remain zero by the classical evolution. See section 2.

In the quantum treatment there are in general other two ways of reaching the global minimum region: one is tunneling through the barrier and the second is allowing to circumvent the maxima by increasing the quantum probability of finding large values of the transverse field components. The tunneling is suppressed in the large N limit because it is related to the quantum effects in the longitudinal directions which are subleading for large N (see comments in section 3.1). In the large N limit the leading quantum effects come from the transversal field components and those are which we describe.

In the early (classical like) dynamics, $\eta(\tau)$ oscillates between η_0 and η_t given by Eq. (19) (see Fig. 7). Thus, as $g\Sigma(\tau) = 0$ the effective mass oscillates between the values (see Figs.

8, 9),

$$\mathcal{M}_{max}^2 = -1 + \eta_0^2 = j - \frac{1}{2}j^2 + \frac{5}{8}j^3 - j^4 + O(j^5) > 0 \quad (33)$$

$$\mathcal{M}_{min}^2 = -1 + \eta_t^2 = -3j - \frac{1}{2}j^2 - \frac{23}{8}j^3 - 4j^4 + O(j^5) < 0 \quad (34)$$

Therefore, the low momentum modes grow exponentially in the time intervals where the effective mass is negative. This spinodal instability increases $g\Sigma(\tau)$ yielding a non-zero probability for the transverse field components.

These instabilities are well approximated by considering a constant negative squared mass $-\mu^2$ given by the average

$$-\mu^2 \simeq \frac{\mathcal{M}_{min}^2 + \mathcal{M}_{max}^2}{2} = -j - \frac{1}{2}j^2 - \frac{9}{8}j^3 - \frac{5}{2}j^4 + O(j^5) \quad (35)$$

This approximation reproduces the growth of $g\Sigma(\tau)$ in good agreement with the full numerical solution of Eqs. (29)–(31) (see appendix 6.1)

$$g\Sigma(\tau) \approx \frac{g\sqrt{\mu\pi}}{8} \frac{e^{2\tau\mu}}{\tau^{3/2}}. \quad (36)$$

Thus the probability of finding large values for the transverse field components increases with time.

This solution holds till a time τ_s (spinodal time) when $g\Sigma(\tau_s) \sim \mu^2$, this condition gives τ_s as the solution of

$$\tau_s \approx \frac{1}{2\mu} \log\left(\frac{8}{g\sqrt{\pi}}\right) + \frac{3}{4\mu} \log(\mu\tau_s) = \frac{1}{2\mu} \log\left(\frac{8}{g\sqrt{\pi}}\right) + \frac{3}{4\mu} \log\left[\frac{1}{2} \log\left(\frac{8}{g\sqrt{\pi}}\right)\right] + \mathcal{O}\left(\frac{\log\log\frac{1}{g}}{\log\frac{1}{g}}\right). \quad (37)$$

After τ_s the effect of $g\Sigma(\tau)$ in the evolution equations become crucial.

Soon after $\tau = \tau_s$ the order parameter $\eta(\tau)$ makes a spectacular jump and starts to oscillate near the global minimum [see Figs. 6, 7]. This transition is explained by the fact that $g\Sigma(\tau) = \frac{\lambda}{2|m|^2} \langle \pi^2(t) \rangle_R \sim 1$ implies transverse field components of the order $|m|/\sqrt{\lambda}$. These large transverse field fluctuations allow the system to turn around the maximum at $\vec{\Phi} = (\sqrt{N}\phi, \vec{\phi}_\pi) = (|m|\sqrt{\frac{2}{\lambda}}\eta_{M'}, \vec{0})$ and reach the region around the global minimum where it oscillates quasi-periodically (see Figs. 6, 7–11).

The growth of $g\Sigma(\tau)$ allows $\eta(\tau)$ to reach the region around the global minimum. That is, the growth of the transverse quantum fluctuations eliminate the barrier that keeps $\eta(\tau)$ near the metastable minimum.

3.3 Intermediate time quantum evolution

After the early period described in the previous section, the system enters in a quasi-periodic regime. Recall that for different initial conditions the oscillations damped much faster [7, 8].

The quasi-periodic regime behaviour found for $\eta(\tau)$ and $g\Sigma(\tau)$ suggests that these quantities are approximately governed by an effective hamiltonian with a few degrees of freedom. Actually, we observe from the full numerical solution of Eqs. (29)–(31) that $g\Sigma(\tau)$ and $\eta(\tau)$ turn to be approximately related as

$$g\Sigma(\tau) = 1 + \alpha j - (1 - \beta j)[\eta(\tau) + j]^2 \quad (38)$$

where α and β are positive numbers of the order j^0 and g^0 for small g . The coefficients α and β are obtained by fitting to the numerical solution. See Table 1.

j	0.05	0.10	0.15	0.20	0.24	0.25	0.30
α	0.74	0.67	0.60	0.56	0.35	0.29	0.18
β	1.36	0.91	0.60	0.40	0.42	0.49	0.43

Table 1: α and β values obtained fitting $g\Sigma(\eta)$ in the time interval $\tau \in [800, 1000]$ for $g = 10^{-6}$ and various j values.

We thus find for the effective squared mass,

$$\mathcal{M}^2(\eta) = -1 + \eta^2 + g\Sigma(\eta) = j \left[\alpha - j + \beta j^2 - 2(1 - \beta j) \eta + \beta \eta^2 \right] \quad (39)$$

The evolution equations (29)–(30) in this approximation take then the form,

$$\ddot{\eta} + \mathcal{M}^2(\eta) \eta = -j \quad (40)$$

We find integrating on η ,

$$\frac{1}{2}\dot{\eta}^2 + j V_{int}(\eta) = j E_{int} \quad (41)$$

where,

$$V_{int}(\eta) = \eta + \frac{1}{2}(\alpha - j + \beta j^2)\eta^2 - \frac{2}{3}(1 - \beta j)\eta^3 + \frac{\beta}{4}\eta^4, \quad (42)$$

$$E_{int} = V_{int}(\eta_1) \quad (43)$$

Notice that E_{int} depends on the initial conditions, and that η_1 is a turning point of the motion. Eq. (41) can be integrated as follows,

$$\sqrt{2j}(\tau - \tau_1) = \int_{\eta_1}^{\eta} \frac{d\eta}{\sqrt{E_{int} - V_{int}(\eta)}} \quad (44)$$

with $\eta_1 = \eta(\tau_1)$.

The fourth order polynomial $E_{int} - V_{int}(\eta)$ has always two real roots $\eta_1 < \eta_2$ corresponding to the turning points. Depending on the value of j , the two other roots are a complex conjugated pair or two more real roots. For each case:

- i) a pair of complex conjugate roots $\eta_R \pm i\eta_I$. We then define:

$$a \equiv \frac{\eta_R - \eta_1}{(\eta_R - \eta_1)^2 + \eta_I^2} ; \quad b \equiv \frac{\eta_I}{(\eta_R - \eta_1)^2 + \eta_I^2} . \quad (45)$$

- ii) a pair of real roots $\eta_1 < \eta_2 < \eta_3 < \eta_4$. We then define:

$$a \equiv \frac{2}{\eta_3 - \eta_1} - \frac{1}{\eta_4 - \eta_1} ; \quad b^2 \equiv \frac{4(\eta_3 - \eta_2)(\eta_4 - \eta_3)}{(\eta_2 - \eta_1)(\eta_4 - \eta_1)(\eta_3 - \eta_1)^2} . \quad (46)$$

We also introduce two other quantities to simplify the formulae:

$$d \equiv \frac{1}{\eta_2 - \eta_1} ; \quad X \equiv \left[(a - d)^2 + b^2 \right]^{1/4} ; \quad C \equiv X \sqrt{2|\mathcal{M}^2(\eta_1) \eta_1 + j|} \quad (47)$$

It is convenient to use in Eq. (44) as integration variable $u \equiv \frac{1}{\eta - \eta_1}$.

The solution of Eq. (44) can be expressed after calculation as

$$\eta(\tau) = \eta_1 + \frac{(\eta_2 - \eta_1)[1 - \text{cn}(C(\tau - \tau_1), k)]}{1 + (\eta_2 - \eta_1)X^2 - [1 - (\eta_2 - \eta_1)X^2] \text{cn}(C(\tau - \tau_1), k)} , \quad (48)$$

where $\text{cn}(z, k)$ is the Jacobi cosine function, and

$$k = \frac{1}{\sqrt{2}} \sqrt{1 + \frac{a - d}{X^2}} \quad (49)$$

the elliptic modulus.

The solution (48) oscillates between η_1 and η_2 with period

$$T = \frac{2}{C} K(k) \quad (50)$$

where $K(k)$ stands for the complete elliptic integral of the first kind and C is given by Eq. (47). The analytical and the numerical solutions are compared in Fig. 11.

The numerical solution would be exactly periodic if E_{int} were exactly conserved; however it is slowly decreasing. The damping is small the smaller is j . See Table 2.

τ	500	1000	1500	2000
$j E_{int}(j = 0.05)$	0.02	0.016	0.014	0.011
$j E_{int}(j = 0.20)$	0.04	0.025	0.015	0.010

Table 2: E_{int} for $g = 10^{-6}$ and $j = 0.05$ and 0.20 .

Thus, E_{int} slowly decreases while $\eta(\tau)$ and $\mathcal{M}^2(\eta)$ oscillate fast showing a clear separation between slow and fast variables. We have explicitly found the fast time dependence of the

order parameter and the quantum fluctuations in terms of elliptic functions. Comparison with the full numerical solution shows that Eqs. (38) and (48) actually reproduce the full dynamics provided the constant parameters in Eq. (48) become **slow** functions of time. For example, the parameters displayed in Table 1 change by 3 – 4% between $\tau = 500$ and $\tau = 1000$. The study of such slow dynamics is a very interesting problem beyond the scope of this article and that can be solved using Whitham methods [10].

As is known, for $j = 0$ the dynamics is governed by a exactly flat effective potential for $|\eta| < 1$ [7]. Since the slow variables become here slower for $j \rightarrow 0$, they may be governed by an effective potential becoming flat at $j = 0$.

Now, we can obtain analytic expressions for $g\Sigma(\tau)$ and $\mathcal{M}^2(\tau)$ from the relations $g\Sigma(\eta)$ [Eq. (38)] and $\mathcal{M}^2(\eta)$ [Eq. (39)], just using the analytical solution $\eta(\tau)$ [Eq. (48)]. The relation $g\Sigma(\eta)$ indicates that $g\Sigma$ and η oscillate with opposite phase, up to order j terms; $g\Sigma(\eta) = 1 - \eta^2 + O(j)$. This $O(j)$ terms are very important because the j^0 terms cancel in the effective mass, and the j terms make the mass to be different from zero. This has the interesting result of making the time averaged squared mass positive. Such average tends asymptotically to a positive value. [Recall that for $j = 0$ in the broken symmetry case the squared mass goes to zero for initial energies below the potential at the local maximum ($\eta = 0$) [7, 8].]

The effective mass vanishes asymptotically for $j \rightarrow 0$. This can be seen explicitly from Eq. (39); it implies $\mathcal{M}^2(\tau = \infty) = \mathcal{O}(j)$ for small j .

Notice also that in the $j = 0$ case the effective mass vanishes asymptotically [7] giving the constraint

$$1 = \eta^2 + g\Sigma \quad \text{for} \quad j = 0 ;$$

and the thick curve in Fig. 10 is $\mathcal{O}(j)$ away from such a parabola; showing that the squared mass is of order j .

The mass of the scalars **around the ground state** \hat{m} follows from the effective potential [see Appendix B]. For $j = 0$ one finds that the mass \hat{m} vanishes [6, 7] in accordance with the presence of $N - 1$ Goldstone bosons. For $j \neq 0$ the mass \hat{m}^2 becomes non-zero and for small j we find in Appendix B,

$$\hat{m}^2 = j + \mathcal{O}(j^2 \log j) \quad \text{for the ground state.}$$

The asymptotic mass squared $\mathcal{M}^2(\infty)$ found above does not coincide with \hat{m}^2 although both masses are of the same order of magnitude $\mathcal{O}(j)$. Notice that \hat{m}^2 describes excitations around the ground state, while $\mathcal{M}^2(\infty)$ corresponds to excitations around states with finite energy density above the ground state.

3.4 Constraints on the trajectory due to the conservation of the energy

As the states considered here are homogeneous and isotropic, the system has an energy-momentum tensor with the ideal fluid form. Thus, we can define a dimensionless energy

as

$$\begin{aligned}
\epsilon &\equiv \frac{\lambda}{2N|m|^4} \langle T^{00} \rangle \\
&= -\frac{\eta^2}{2} + \frac{\eta^4}{4} + \frac{1}{2} \eta^2 g \Sigma - \frac{g \Sigma}{2} + \frac{(g \Sigma)^2}{4} + \frac{1}{4} + j \eta \\
&\quad + \frac{\dot{\eta}^2}{2} + \frac{g}{2} \int q^2 dq |\dot{\varphi}_q|^2 + \frac{g}{2} \int q^2 dq q^2 |\varphi_q|^2 .
\end{aligned} \tag{51}$$

for $\tau > 0$.

The conservation of the energy (for constant external fields) gives us the following constraint in the $(\eta, g\Sigma)$ plane

$$\epsilon_0 \geq V_{eff\ dyn}(\eta, \Sigma) \equiv -\frac{\eta^2}{2} + \frac{\eta^4}{4} + \frac{1}{2} \eta^2 g \Sigma - \frac{g \Sigma}{2} + \frac{(g \Sigma)^2}{4} + \frac{1}{4} + j \eta . \tag{52}$$

where $\epsilon_0 = V_{\tau \leq 0}(\eta_0) + 2j\eta_0 = V_{\tau > 0}(\eta_0)$ is the energy after the sign change in the external field j .

This constraint is represented as a dotted line in Fig. 10. We see there how the energy conservation constrains the trajectories in the $(\eta, g\Sigma)$ plane.

$V_{eff\ dyn}(\eta, \Sigma)$ can be interpreted as a dynamical effective potential for the longitudinal field η . Notice that the equation of motion (29) for $\eta(\tau)$ can be written as

$$\ddot{\eta}(\tau) = -\frac{\partial}{\partial \eta} V_{eff\ dyn}(\eta, \Sigma) .$$

$V_{eff\ dyn}(\eta, \Sigma)$ defined by eq. (52) is plotted for $j = 0.20$ in Fig. 12.

4 Comments and Conclusions

Here, we have studied effects of external fields in non-perturbative quantum field dynamics in the large N limit. The effects of uniform external fields in Φ^4 theory with broken symmetry were recently studied in a different framework through classical evolution with random initial conditions [11].

We have studied the evolution of the ground state in an external uniform field J after flipping its sign: $J \rightarrow -J$. We have considered the broken symmetry case and small external fields (then the classical potential presents two local minima).

The change of sign in the external field leads to spinodal instabilities and parametric resonances yielding abundant particle creation of the order $1/\lambda$. As a consequence, the wave functional spreads allowing large values for field components orthogonal to $\vec{\mathcal{J}}$. Thanks to such large transverse field fluctuations the system goes around the maximum of the potential and reaches the global minimum without tunneling.

The large transverse fluctuations $\Sigma(\tau)$ change the effective mass squared in the evolution of the longitudinal field $\eta(\tau)$ [see eqs.(29)-(30)]. In this way $\eta(\tau)$ overcomes the classical

barrier and reaches the absolute minimum. The effective dynamical potential $V_{eff\ dyn}(\eta, \Sigma)$ introduced in eq.(52) helps to understand this phenomenon. As shown in fig. 12, the barrier in the η direction between the two minima of $V_{eff\ dyn}(\eta, \Sigma = 0)$ disappears in $V_{eff\ dyn}(\eta, \Sigma)$ for sufficiently large Σ .

After that, the system oscillates reaching an almost periodic regime. That is, fast variables (whose time evolution we explicitly solve) oscillate periodically while other variables change slowly due to a tiny damping.

In this quasi-periodic regime the effective squared mass is of order J . Thus, in the $J \rightarrow 0$ limit we recover a zero effective squared mass consistently with the known results for $J = 0$ where out of equilibrium Goldstone bosons appear [7, 8].

The damping of the fast oscillations is here much slower than for the oscillations found in refs. [7, 8] for other initial conditions. There, the oscillations of $\mathcal{M}^2(t) - \mathcal{M}^2(\infty)$ were damped as $1/t$, while the damping is significantly slower for the quasi-periodic solutions found here.

5 Acknowledgements

We thank Andras Patkós for useful discussions before this work was started and Daniel Boyanovsky for useful comments.

6 Appendix

6.1 Appendix A: Spinodal instability

Here, we obtain the early time solution for the modes in the spinodally resonant band, and we estimate the spinodal time, τ_s .

Before entering on the calculation of τ_s , let us recall that the contribution of the spinodal band can be estimated using an average mass for the evolution. The numerical calculations show that this estimation is correct, until such contribution becomes of order one.

Hence, an approximate equation for the modes reads,

$$\left(\frac{d^2}{d\tau^2} + q^2 - \mu^2 \right) \varphi_q(\tau) = 0 . \quad (53)$$

The modes with q in the interval between 0 and μ are spinodally resonant. There are no particles in the spinodally resonant band. Therefore the initial condition for modes in the resonant band are:

$$\varphi_q(0) = \frac{1}{\sqrt{\Omega_q}} = \left(q^2 + |\mathcal{M}^2(0)| \right)^{-1/4}, \quad \dot{\varphi}_q(0) = -i\sqrt{\Omega_q} = -i \left(q^2 + |\mathcal{M}^2(0)| \right)^{1/4}. \quad (54)$$

The solution of Eq. (53) for these modes is:

$$\varphi_q(\tau) = \frac{1}{2\sqrt{\mu^2 - q^2}(q^2 + |\mathcal{M}^2(0)|)^{1/4}} \left[\left(\sqrt{\mu^2 - q^2} - i\sqrt{q^2 + |\mathcal{M}^2(0)|} \right) e^{\tau\sqrt{\mu^2 - q^2}} + \left(\sqrt{\mu^2 - q^2} + i\sqrt{q^2 + |\mathcal{M}^2(0)|} \right) e^{-\tau\sqrt{\mu^2 - q^2}} \right]. \quad (55)$$

We thus obtain for the squared modulus neglecting the exponentially decreasing term

$$|\varphi_q(\tau)|^2 \approx \frac{\mu^2 + |\mathcal{M}^2(0)|}{4\mu^2 \left(1 - \frac{q^2}{\mu^2}\right) \sqrt{q^2 + |\mathcal{M}^2(0)|}} e^{2\tau\mu\sqrt{1 - \frac{q^2}{\mu^2}}}. \quad (56)$$

The contribution of the spinodal band to $g\Sigma(\tau)$ is given by,

$$\Sigma_s(\tau) = \int_0^\mu q^2 dq |\varphi_q(\tau)|^2. \quad (57)$$

Inserting Eq. (56) into Eq. (57) we obtain an estimation for the spinodal growth of the quantum fluctuations. To approximately evaluate this integral, we can make further simplifications in Eq. (56). As $q/\mu < 1$ and the contribution of the modes with $q \approx \mu$ is exponentially suppressed, we can expand in q/μ to second order in the exponential and to zeroth order in the factor outside the exponential.

$$|\varphi_q(\tau)|^2 \approx \frac{\mu^2 + |\mathcal{M}^2(0)|}{4\mu^2 \sqrt{q^2 + |\mathcal{M}^2(0)|}} e^{2\tau\mu} e^{-\tau\frac{q^2}{\mu}}. \quad (58)$$

In addition, the integrand has its maximum at $q = O(0.1\mu)$ and $0 < \mu < 1$. Therefore, we can approximate $\mu^2 + |\mathcal{M}^2(0)| \sim 2\mu^2$ and $\sqrt{q^2 + |\mathcal{M}^2(0)|} \sim \mu$. Thus,

$$|\varphi_q(\tau)|^2 \approx \frac{1}{2\mu} e^{2\tau\mu} e^{-\tau\frac{q^2}{\mu}}. \quad (59)$$

Then integrating over q and using $\int_0^1 v^2 dv \exp(-v^2 r) \xrightarrow{r \rightarrow \infty} \sqrt{\pi/(16r^3)}$,

$$g\Sigma(\tau) \approx \frac{g\sqrt{\pi\mu}}{8} \frac{e^{2\tau\mu}}{\tau^{3/2}}. \quad (60)$$

The spinodal time τ_s is, by definition, the time where the instabilities are shut off for all $0 \leq q \leq \mu$. This happens when the spinodal modes contribution $g\Sigma_s(\tau)$ compensates the initial (negative) value of $M_{eff}^2(\tau) = -\mu^2$.

$$g\Sigma_s(\tau_s) \approx \mu^2 \quad (61)$$

Therefore τ_s is given by the following implicit equation,

$$\tau_s = \frac{1}{2\mu} \log \left[\frac{8}{g\sqrt{\pi}} \right] + \frac{3}{4\mu} \log(\mu\tau_s). \quad (62)$$

The spinodal times given by this equation are in good agreement with the numerical results.

6.2 Appendix B: Ground state results

The expectation value of the field φ and the mass of the scalars can be obtained for the ground state using the effective potential [6, 7]. One finds in the broken symmetry case using dimensionless variables,

$$\varphi^2 = 1 + \hat{m}^2 + \frac{\lambda \hat{m}^2}{2(4\pi)^2} \log \frac{1}{\hat{m}^2} ,$$

where \hat{m} is the mass around the ground state of the $N - 1$ scalars. The field expectation value is connected with the external source by [6, 7]

$$\varphi = \frac{j}{\hat{m}^2} .$$

Hence, \hat{m}^2 is a function of j defined by the trascendental equation

$$\hat{m}^2 \sqrt{1 + \hat{m}^2 + \frac{\lambda \hat{m}^2}{2(4\pi)^2} \log \frac{1}{\hat{m}^2}} = j . \quad (63)$$

For $j = 0$ one finds that $\hat{m} = 0$ in accordance with the presence of $N - 1$ Goldstone bosons. For $j \neq 0$ the mass \hat{m}^2 becomes non-zero and for small j we find

$$\hat{m}^2 = j + \mathcal{O}(j^2 \log j) \quad \text{for the ground state.}$$

[Notice that Eq.(63) becomes the classical equation Eq.(10) for $\lambda = 0$ setting $\hat{m}^2 = -1 + \eta^2$, as expected.]

References

- [1] J. W. Harris, B. Muller, Annu. Rev. Nucl. Part. Sci. **46**, 71 (1996);
 B. Muller in *Particle production in Highly Excited Matter*, Eds. H. H. Gutbrod, J. Rafelski, NATO ASI series B, vol. 303 (1993);
 B. Muller, *The Physics of the Quark Gluon Plasma* Lecture Notes in Physics, Vol. 225, Springer-Verlag, Berlin, Heidelberg, 1985;
 K. Geiger, Phys. Rep. **258**, 237 (1995); Phys. Rev. **D46**, 4965 (1992); Phys. Rev. **D47**, 133 (1993); *Quark Gluon Plasma 2*, Ed. by R. C. Hwa, World Scientific, Singapore, 1995.
 X. N. Wang, Phys. Rep. **280**, 287 (1997)
 M. H. Thoma, in *Quark Gluon Plasma 2*, Ed. by R. C. Hwa, World Scientific, Singapore, 1995.
 Robert D. Pisarski, *Nonabelian Debye screening, tsunami waves, and worldline fermions* in the Proceedings of the International School of Astrophysics D. Chalonge, p. 195, eds. N. Sánchez, A. Zichichi, Kluwer Acad. Publ., Dordrecht, 1998.

- [2] See for example, D. Boyanovsky and H. J. de Vega, p. 37, ‘Currents Topics in Astro-fundamental Physics: the Cosmic Microwave Background’, Proceedings of the VIIth. Erice Chalonge School N. Sánchez editor, Kluwer, NATO ASI Series C, 2000, [astro-ph/0006446].
- [3] D. Boyanovsky, H. J. de Vega and R. Holman, Phys. Rev. **D49**, 2769 (1994).
D. Boyanovsky, D. Cormier, H. J. de Vega, R. Holman, A. Singh, M. Srednicki, Phys. Rev. **D56**, 1939 (1997).
- [4] D. Boyanovsky, F. J. Cao, H. J. de Vega, *Inflation from tsunami-waves*, astro-ph/0102474.
- [5] D. Boyanovsky, H. J. de Vega and R. Holman and J. Salgado, Phys. Rev. **D54**, 7570 (1996).
- [6] S. Coleman, R. Jackiw and H. D. Politzer, Phys. Rev. D 10, 2491 (1974). L. F. Abbott, J. S. Kang and H. J. Schnitzer, Phys. Rev. D 13, 2212 (1976).
- [7] D. Boyanovsky, H. J. de Vega and R. Holman and J. Salgado, Phys. Rev. **D59**, 125009 (1999).
- [8] F. J. Cao, H. J. de Vega, Phys. Rev. **D63**, 045021 (2001).
- [9] S. Habib, Y. Kluger, E. Mottola, J. P. Paz, Phys. Rev. Lett. **76** (1996) 4660.
- [10] G. B. Whitham, ‘Linear and nonlinear waves’, John Wiley, 1974.
- [11] Sz. Borsányi, A. Patkós, J. Polonyi, Zs. Szép, Phys. Rev. **D62**, 085013 (2000).
Sz. Borsányi, Zs. Szép, hep-ph/0011283.
Sz. Borsányi, A. Patkós, D. Sexty, Zs. Szép, hep-ph/0105332.

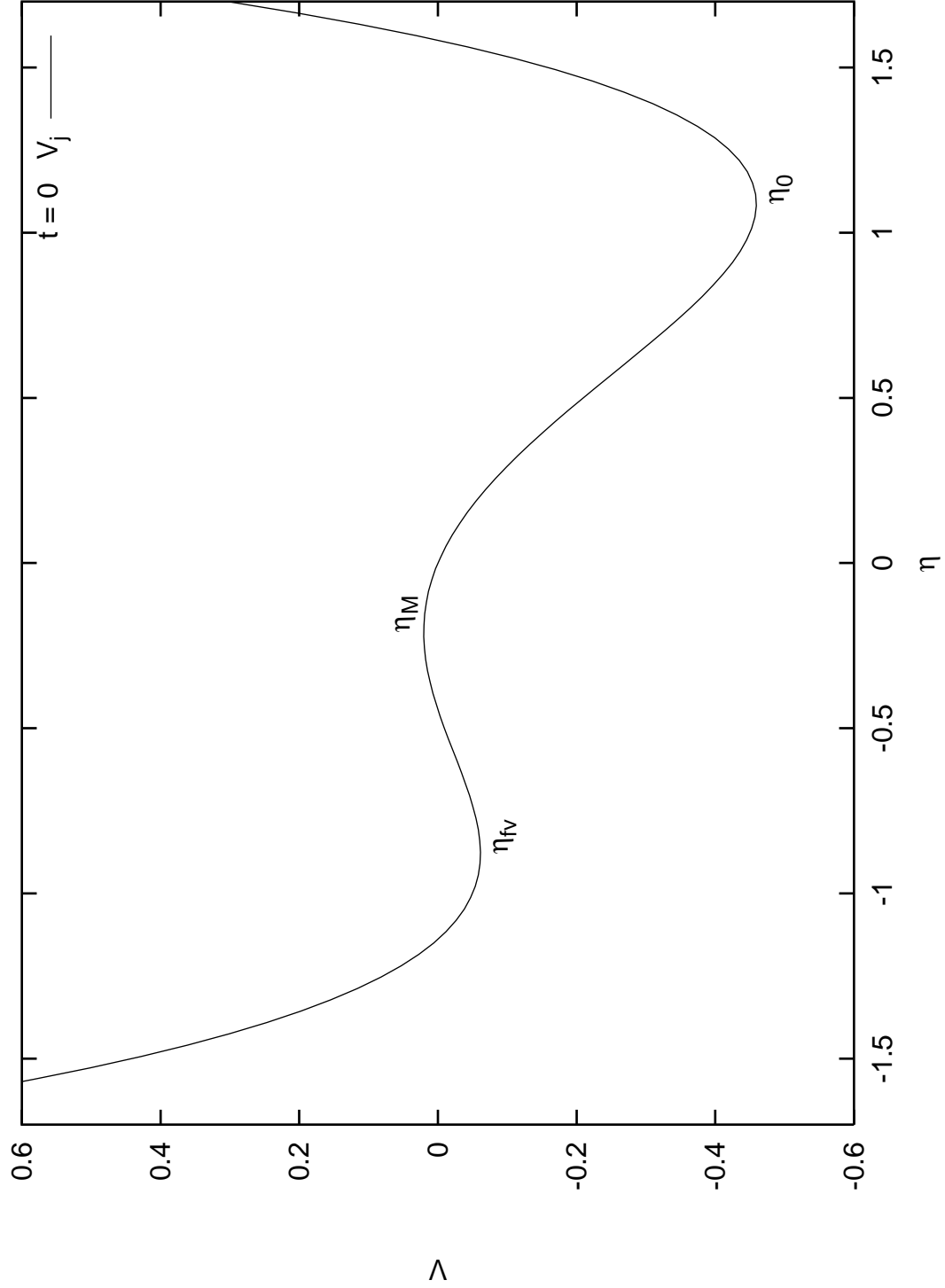


Figure 1: Classical potential at $\tau \leq 0$ for small field $j = 0.20 < 2/\sqrt{27}$. The potential presents two minima (the ground state η_0 and a metastable false vacuum state η_{fv}) separated by a potential barrier.

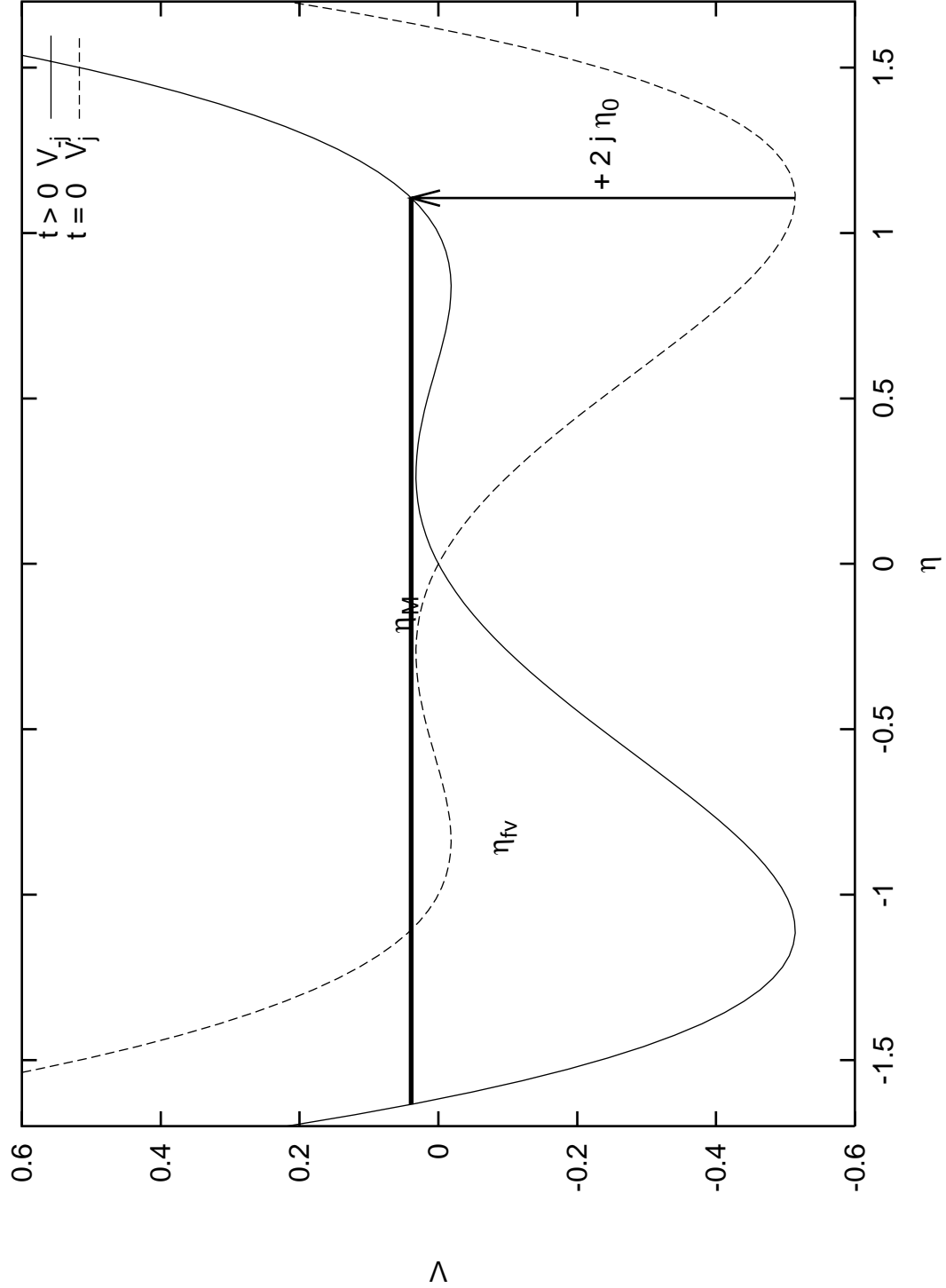


Figure 2: $j = 0.25 > j_c$. Classical potential at $\tau = 0$ and for $\tau > 0$. The change of the sign of the external field at $\tau = 0$ increases in $2j\eta_0$ the energy density of the system, and the system has for $j > j_c$ enough energy to jump above the barrier.

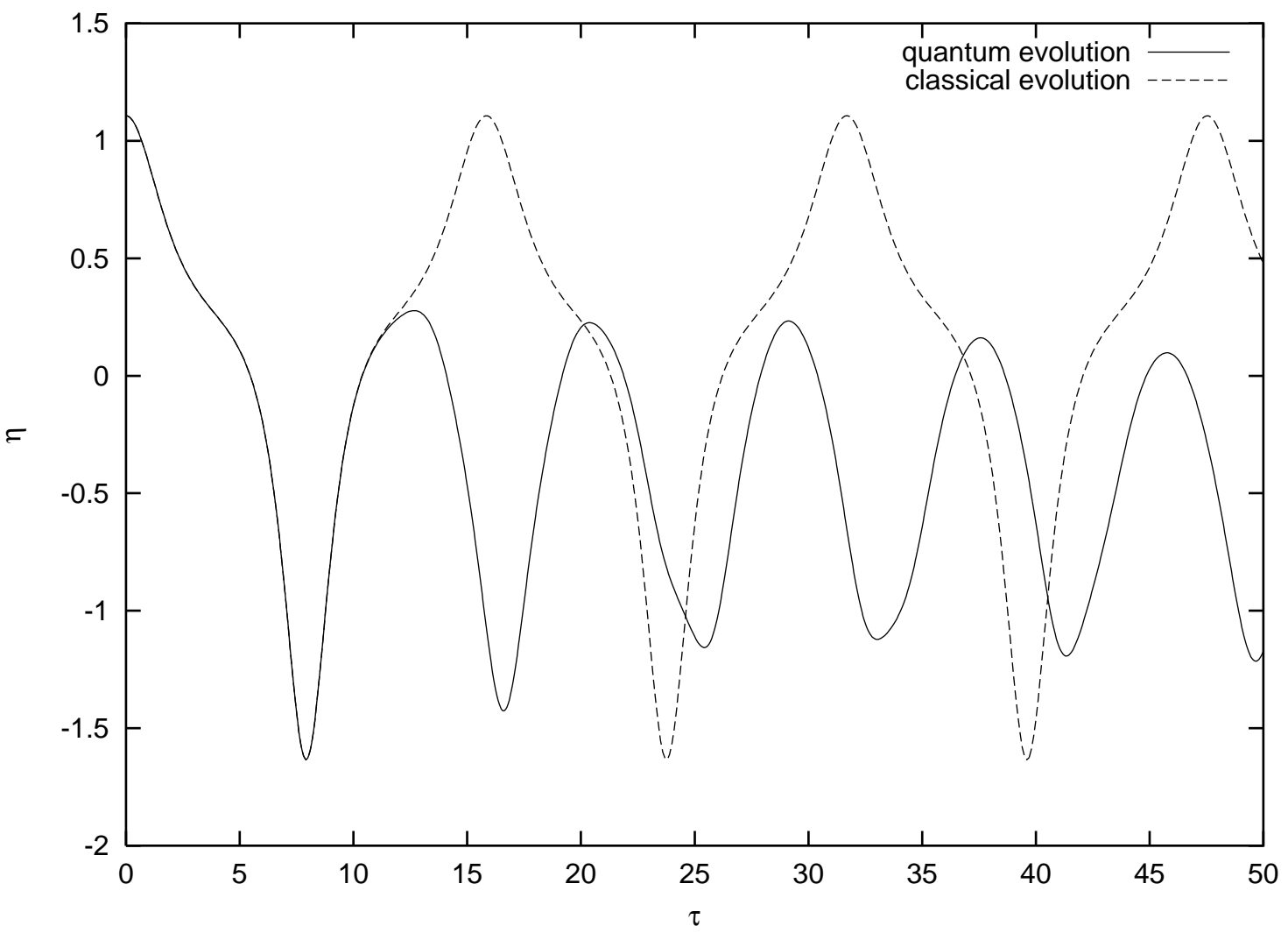


Figure 3: $j = 0.25 > j_c$. $\eta(\tau)$ from the quantum (full line) and the classical (dashed line) evolution.

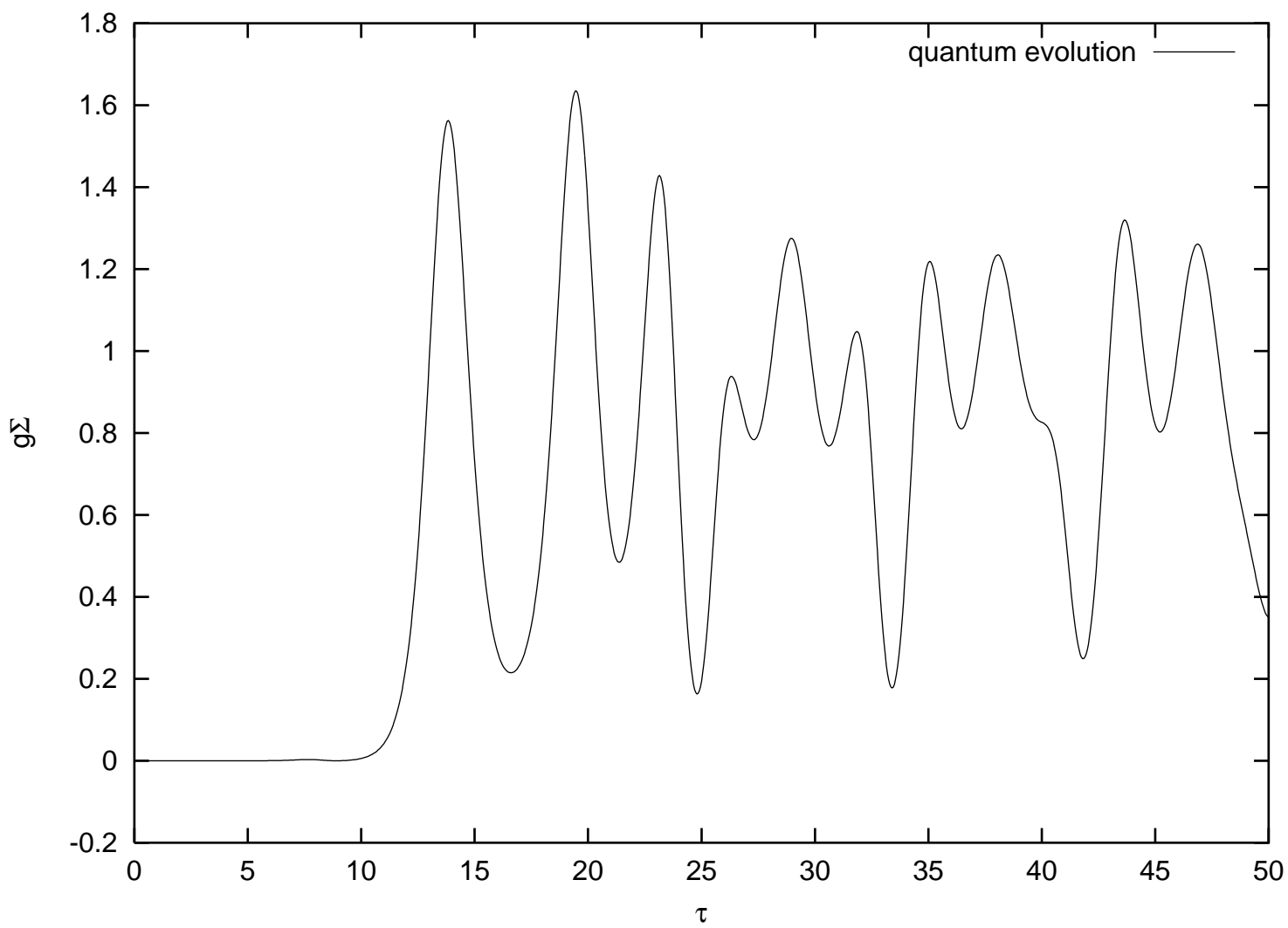
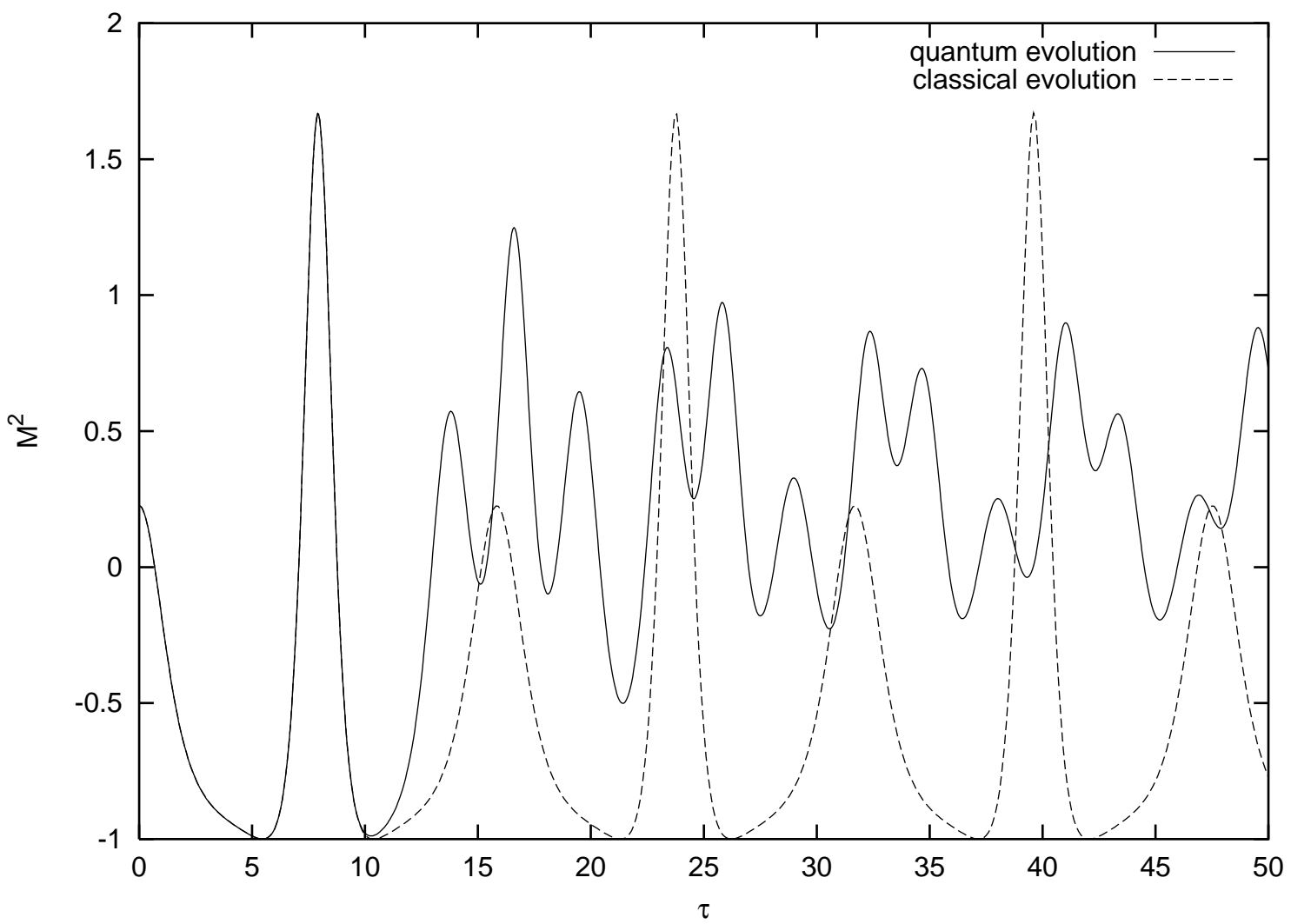


Figure 4: $j = 0.25 > j_c$. $g\Sigma(\tau)$.



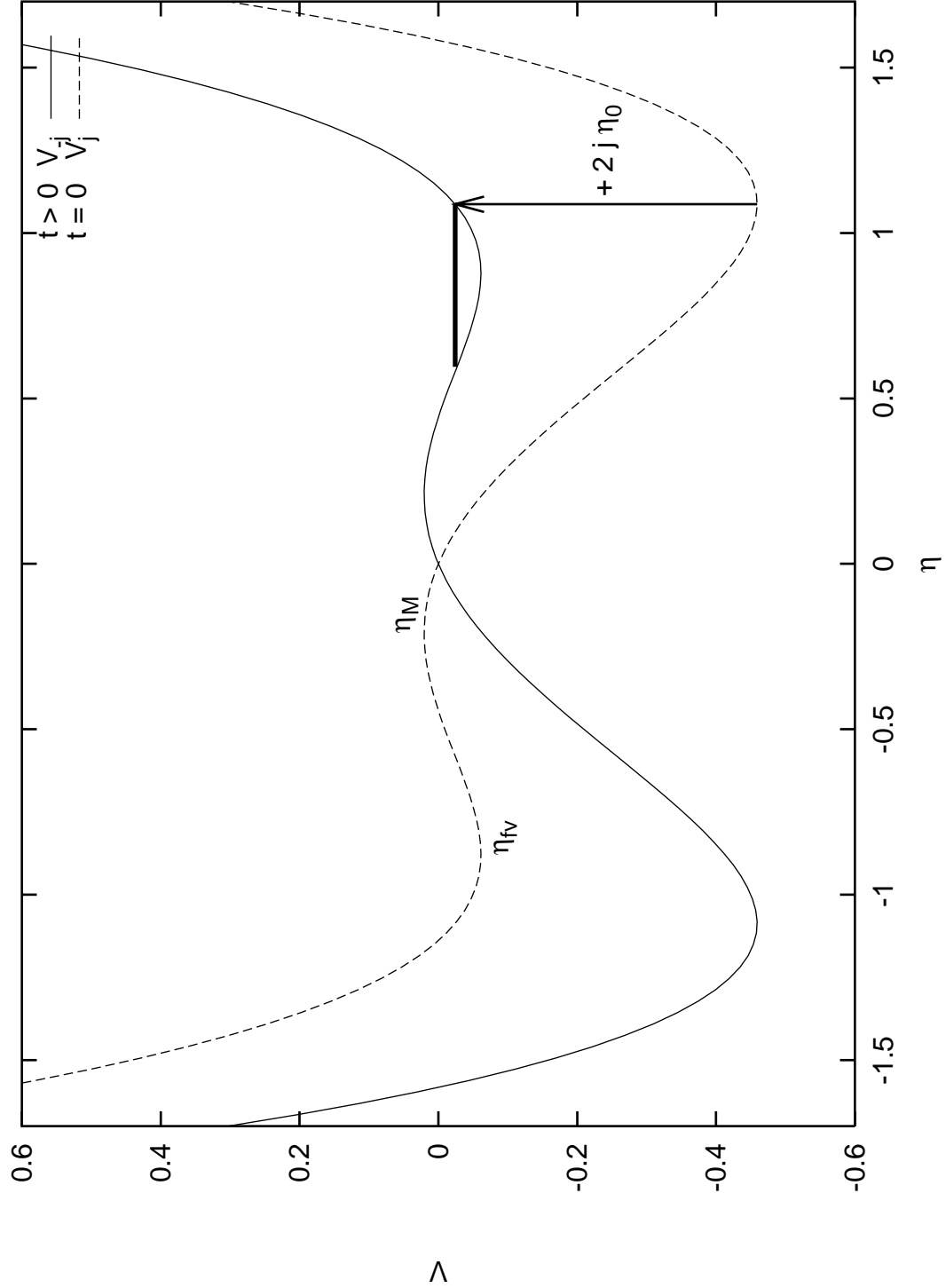


Figure 6: $j = 0.20 < j_c$. Classical potential at $\tau = 0$ and for $\tau > 0$. The change of the sign of the external field at $\tau = 0$ increases in $2j\eta_0$ the energy density of the system but the system **does not** have enough energy to jump above the barrier.

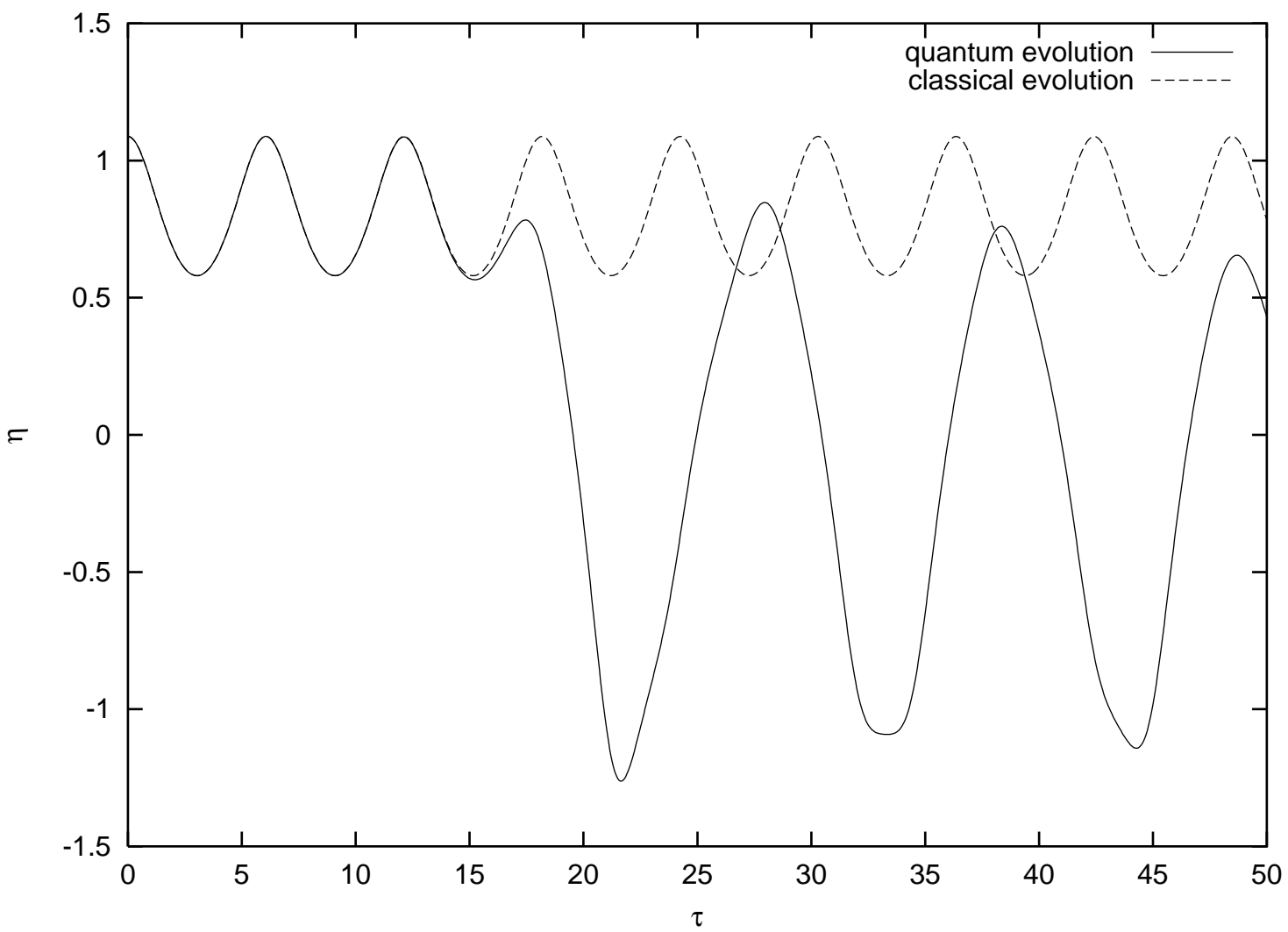


Figure 7: $j = 0.20 < j_c$. $\eta(\tau)$ for the quantum (full line) and for the classical (dashed line) evolution.

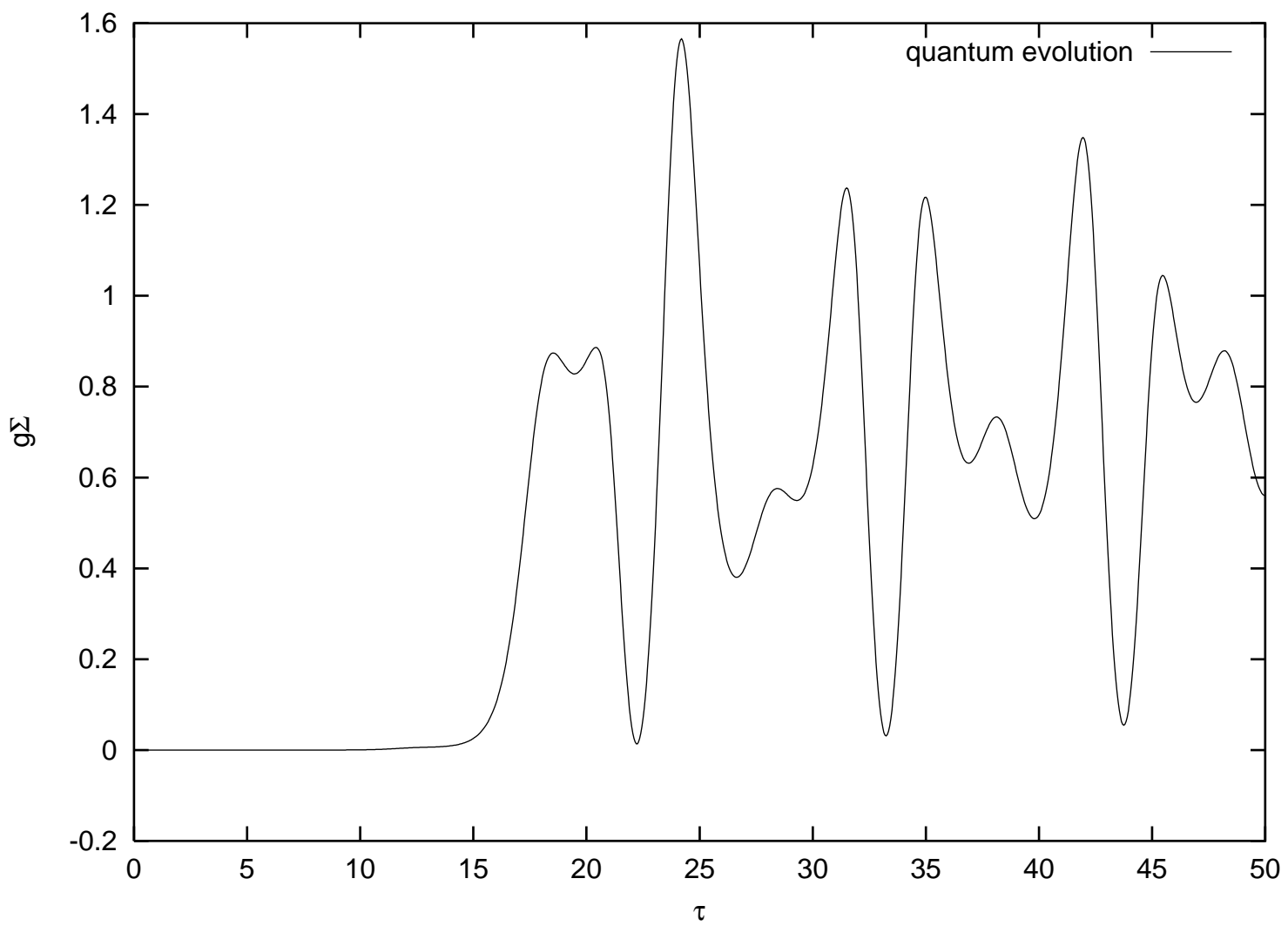


Figure 8: $j = 0.20 < j_c$, $g\Sigma(\tau)$.

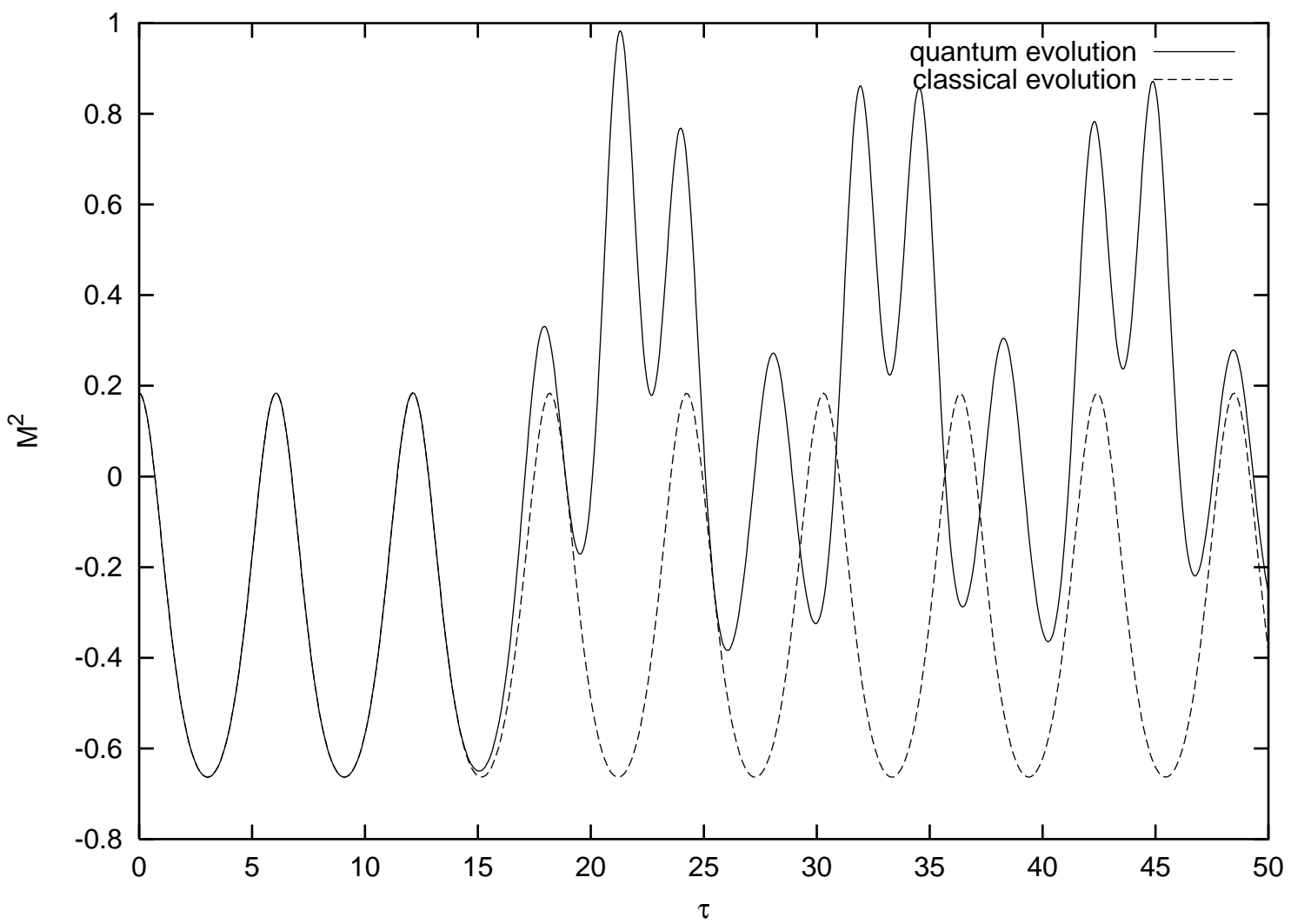


Figure 9: $j = 0.20 < j_c$. Effective mass squared $M^2(\tau)$ for the quantum (full line) and for the classical (dashed line) evolution.

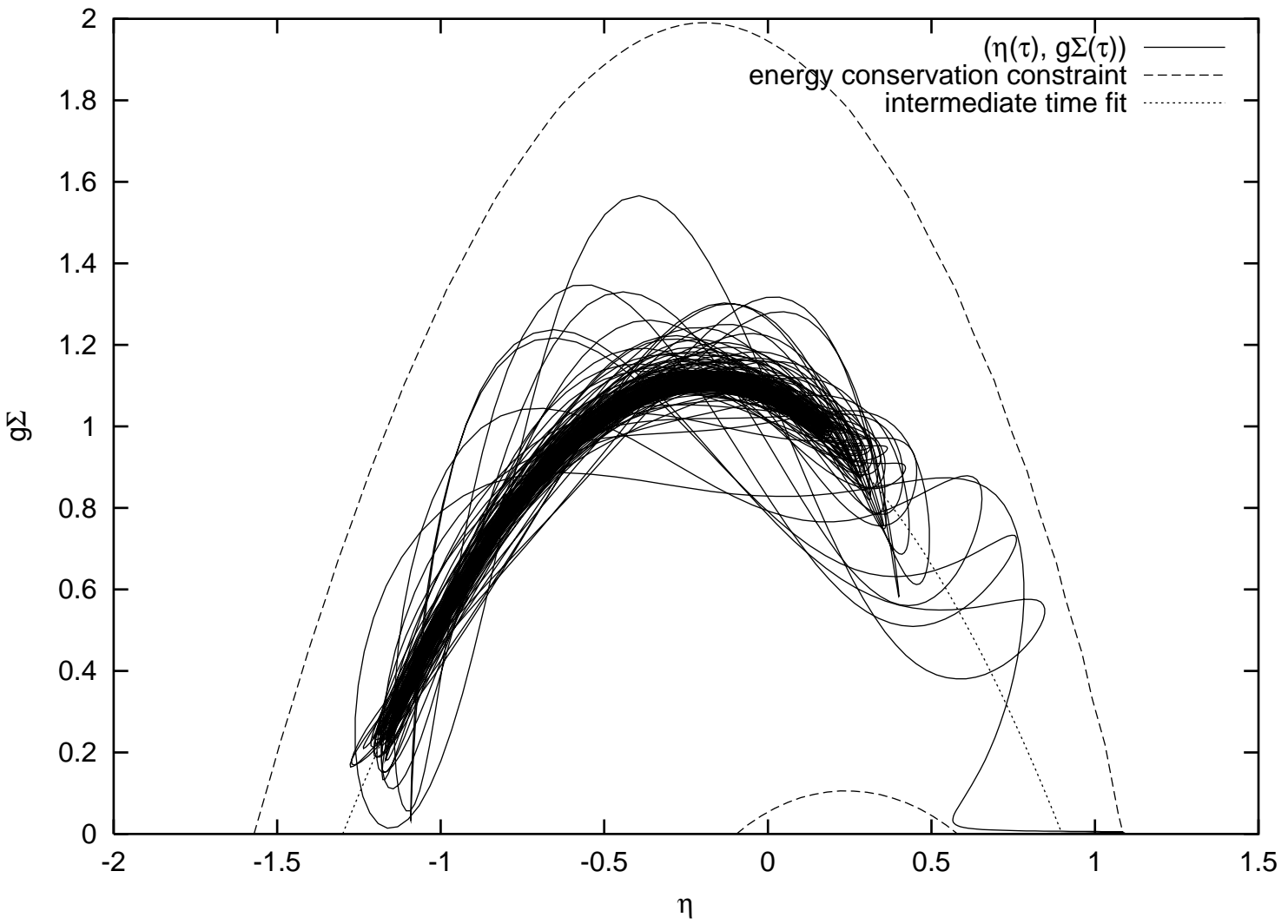


Figure 10: $j = 0.20 < j_c$. Full line: trajectory in the $(\eta, g\Sigma)$ plane. Dotted line: constraint in the trajectory due to the energy conservation. See Eq. (52) and Fig. 12.

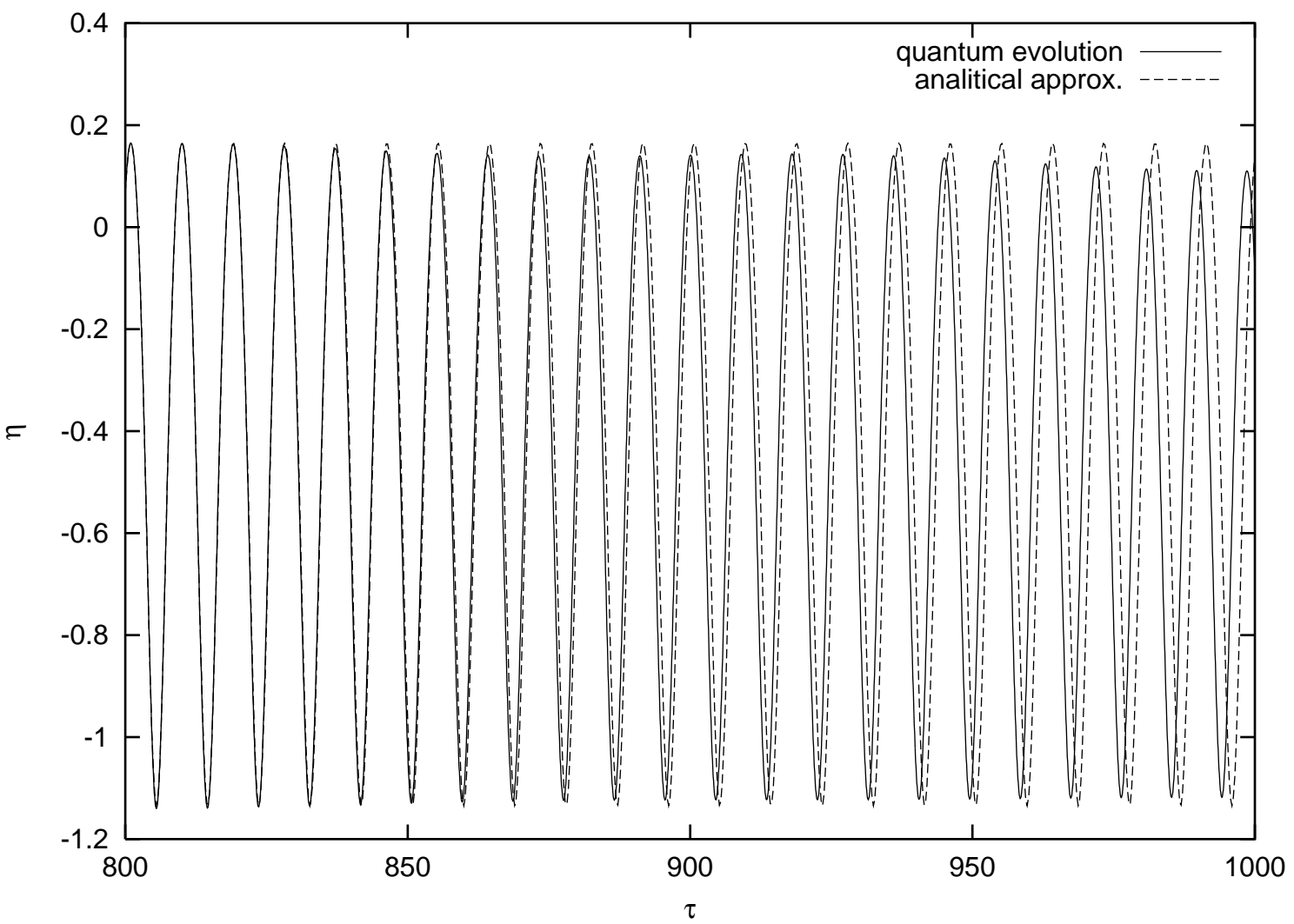


Figure 11: $j = 0.20 < j_c$. Quantum evolution for the field expectation value $\eta(\tau)$ (full line) compared to the analytical intermediate time approximation (dashed line).

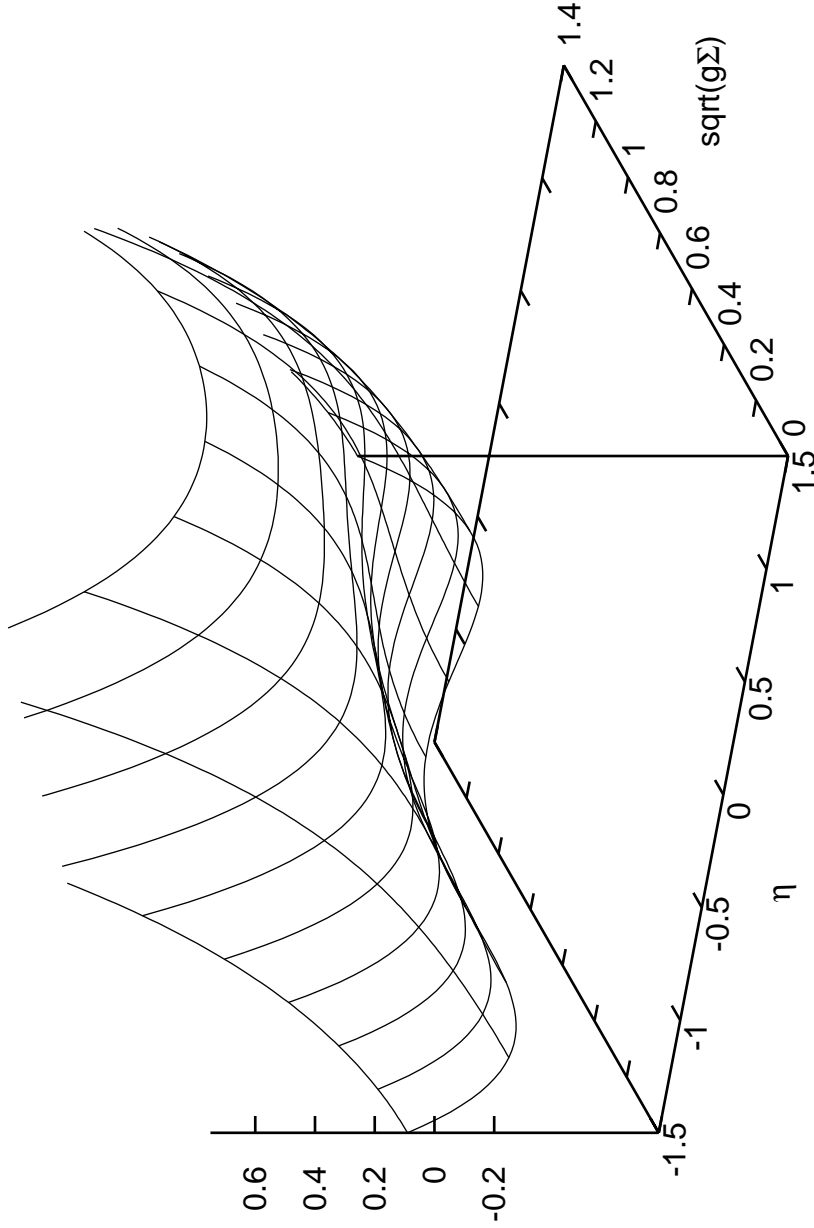


Figure 12: $j = 0.20 < j_c$. Plot of the dynamical effective potential $V_{eff\ dyn}(\eta, \Sigma)$ given by eq.(52). $V_{eff\ dyn}(\eta, \Sigma)$ is bounded from above by the total energy. This constrains the trajectory represented in Fig. 10.